Estimation of an object's physical parameter by force sensors of a dual-arm robot

Sheng, CAO
Zhiwei, LUO
Changqin, QUAN

(Citation)
Journal of Mechanics Engineering and Automation,7(3):120-131

(Issue Date)
2017

(Resource Type)
journal article

(Version)
Version of Record

(URL)
https://hdl.handle.net/20.500.14094/90006861

Journal of Mechanics Engineering and Automation 7 (2017) 120-131
doi: 10.17265/2159-5275/2017.03.002

Estimation of an Object's Physical Parameter by Force Sensors of a Dual-arm Robot

CAO Sheng, LUO Zhiwei and QUAN Changqin

Graduate School of System Informatics, Kobe University, 1-1 Rokkodai-cho, Nada-ku, Kobe 657-8501, Japan

Abstract: We are developing a nursing-care robot for physical care tasks. The concept of this robot is to promote the cared persons by the robot to activate their own motion ability as long as possible. This may lead to the improvement of the cared person's movement volition and movement abilities. In order to realize safe and human friendly robot care tasks, full body manipulation is an important technology, for which it is necessary to estimate the subject's center of gravity from the contact positions and forces with the robot's two arms. In this paper, we estimate the center of gravity of object based on the contact point and the contact force estimated by force sensor on both robot arms. The position of gravity center is important to realize care tasks stably. We performed experiments and simulations for the single point contact and dual points contact cases using a cylindrical object. As a result, it is found that although some errors were recognized in the experiments compared with the simulations, the relations between the contact positions and such errors were observed. Such experimental error mainly comes from the difference of shape between the real robot and the model of the robot in simulation.

Key words: Nursing care robot, estimation of physical parameter.

1. Introduction

In the recent years, increase of age population becomes a serious problem in human societies. With the rapid development of the aging population, the elderly people's nursing care becomes more and more serious because of the lack of the care supporters. The research on nursing care robot is one necessary way to solve this problem.

Nursing care robots have been widely studied in recent years [1-5]. The appearance of its beneficial comes from both care supporters as well as cared persons. The nursing care robot can be roughly divided into three types, such as care-assisted type, self-assisted type and communication type.

In order to reduce the burden of cared persons while realizing the action of carrying up care, it is important to clarify their physical conditions using the information from cameras and any other kinds of sensors.

Corresponding author: CAO Sheng, Ph.D., research fields: robot's manipulator control, rehabilitation robot, cable-driven robot.

When the robot is lifting up someone, it is necessary to concern two different purposes of assisting and sustaining to control the dual arm of the robot. Since the force of assisting arm depends on the force of sustaining arm, it is possible to encourage the cared persons to act by themselves instead of depending on the robots totally. In order to determine the force of assisting arm, physical parameters of cared person's body are required.

Since the robot is controlled basing on the measured parameters provided by sensors, how to get the parameters of the care receiver's body without noise is quite important. Nagase [6] proposed a method of estimating a contact point between a robot hand and an object by using a force sensor with measurement noise. He builds an objective function which represented the error and used the Lagrange multipliers to choose an optimal solution which makes error as small as possible.

In another hand, human body is a redundant system due to its lots of D.O.Fs. This makes the computation which serves the control of the care receiver's posture

very difficult. In Ref. [7], Dong reduced the unnecessary D.O.Fs of the human body to make the model be simple. He also proposed an adaptive force control method to handle the model uncertainties. Thus, when we analysed the situation of the person to be lifted up, we can regard his/her body as a simple geometrical shape so that the robot can complete the task at the real time.

In this study, we use 6 axis force sensors to measure the force and moment of the contacted person. Based on the measured force and moment from the force sensors, we estimate the contact position on the robot arm and contact force. From these estimated information and the model of the robot, we estimate the position of the center of gravity of the person to be cared.

Section 2 presents our developed nursing care robot. Section 3 describes the method to estimate the object's physical parameters based on our optimization algorithm. Section 4 and Section 5 perform the simulation and actual experiment and discuss the results.

2. Overview of Robot's Structure

The nursing care robot that we are developing is shown in Fig. 1, where the upper body is designed in a humanoid type with 14 degrees of freedom as shown in Fig. 2. The 14 degrees of freedom contain 2 D.O.F

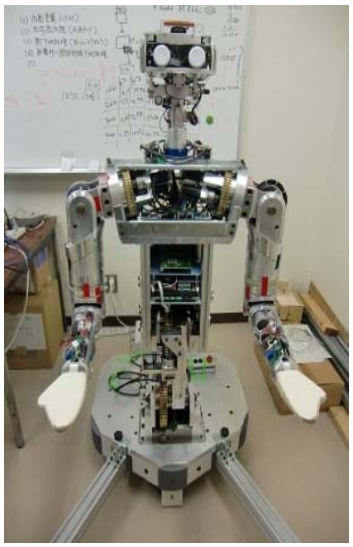

Fig. 1 Nursing-care robot.

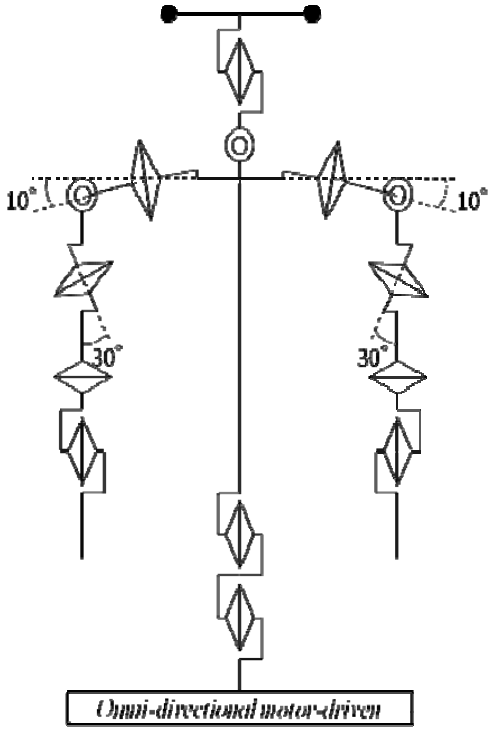

Fig. 2 Degree of freedom of robot.

of the neck joint of the head, 3 D.O.F of shoulders joints both on left and right side, 2 D.O.F of elbow joints both on left and right side, 2 D.O.F of hip joints. The total length of the robot is 1.5 m high with the mass of about 100 kg. Two force sensors with 6 D.O.F. are equipped at the upper arms of the robot.

3. Estimation of an Object's Physical Parameter

3.1 Estimation of the Contact Position When Contact with One Point

3.1.1 The Model and Formulation

In order to estimate the contact position between the robot arm and the object by using 6-axis force sensor which is installed on the upper arm part of the robot, the model can be assumed as Fig. 3.

For simplicity, here the robot arm can be assumed as a cylinder with radius r. The origin of the sensor coordinate system Σ_S is set as the center of the sensor. In addition, there are two coordinate systems of the elbow (the pivot axis coordinate system Σ_E and the flexion axis coordinate system Σ_H). The rotation

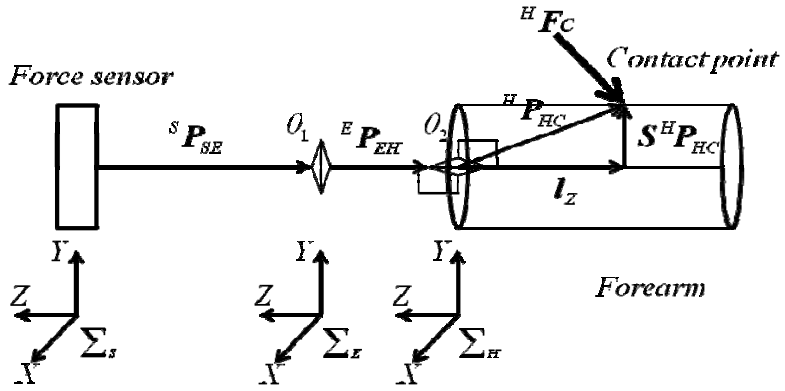

Fig. 3 Contact between a robot arm and an object.

matrix performing coordinate transformation can be represented as ${}^{H}R_{E}$, ${}^{E}R_{S}$. Moreover, the vector from the origin of the flexion axis coordinate system to the contact point and the contact force can be set as ${}^{H}P_{HC}$ and ${}^{H}F_{C}$, respectively. S is a projecting matrix from XYZ space to the XY plane. The force and moment acted on the origin of the flexion coordinate system are represented as ${}^{H}F_{S}$, ${}^{H}M_{f}$. Moreover, ${}^{S}F_{S}$ ${}^{S}M_{f}$ are the force and the moment observed from the origin of the force sensor coordinate. Thus, the coordinate transformation from the sensor coordinate system to the flexion axis coordinate system can be

$$\begin{pmatrix} {}^{H}F_{S} \\ {}^{H}M_{f} \end{pmatrix} = \begin{pmatrix} {}^{H}R_{E} & 0 \\ [{}^{H}P_{EH}\times]\,{}^{H}R_{E} & {}^{H}R_{E} \end{pmatrix} \begin{pmatrix} {}^{E}R_{S} & 0 \\ [{}^{E}P_{SE}\times]\,{}^{E}R_{S} & {}^{E}R_{S} \end{pmatrix} \begin{pmatrix} {}^{S}F_{S} \\ {}^{S}M_{f} \end{pmatrix} \tag{1}$$

If there exists no noise, then

$$\begin{aligned} {}^{H}F_{S} &= {}^{H}F_{C} \\ {}^{H}M_{f} &= {}^{H}P_{HC} \times {}^{H}F_{C} \end{aligned} \tag{2}$$

Since the contact point is on the surface of cylinder, thus

$$g\left(S\,{}^{H}P_{HC}\right) = \left\|S\,{}^{H}P_{HC}\right\|^{2} - r^{2} = 0 \tag{3}$$

Because the contact force only exists on the direction into the cylinder, it is concluded that

$$\left(S\,{}^{H}P_{HC}\right)^{T}\,{}^{H}F_{S} \le 0 \tag{4}$$

Here, ${}^{H}P_{EH}$ and ${}^{E}P_{SE}$ are already known. If there exist some noises, the determination of the contact position ${}^{H}P_{HC}$ becomes a problem.

Since the existence of the noises, the balance of the Eq. (2) has been broken and the error e can be calculated as

$$e = {}^{H}F_{S} \times {}^{H}P_{HC} + {}^{H}M_{f} \tag{5}$$

From Eq. (5), it is obvious that there exists an optimal estimation of ${}^{H}P_{HC}$ minimizing the error value e. We can form an objective function subjected to two constraints to solve error e's minimization problem.

$$\begin{cases} Objective\ Function: & \|e\|^{2} = \left\|{}^{H}F_{S} \times {}^{H}P_{HC} + {}^{H}M_{f}\right\|^{2} \\ S.T. \quad I. & g\left(S\,{}^{H}P_{HC}\right) = \left\|S\,{}^{H}P_{HC}\right\|^{2} - r^{2} = 0 \\ II. & \left(S\,{}^{H}P_{HC}\right)^{T}\,{}^{H}F_{S} \le 0 \end{cases} \tag{6}$$

The method of Lagrange multipliers can be used to solve this optimization problem.

3.2 Derivation of Analytical Solution

Firstly, in order to solve the optimization problem Eq. (6), it is necessary to only consider the objective function and the constraint I. Then, by imposing constraint II, we can get the solution of Eq. (6). The Lagrange function can be formed based on the objective function and constraint I.

$$L = \frac{1}{2}\left\|\left[{}^{H}F_S\times\right]{}^{H}P_{HC} + {}^{H}M_f\right\|^2 + \frac{1}{2}\lambda\left(\left\|S\,{}^{H}P_{HC}\right\|^2 - r^2\right) \quad (7)$$

The first necessary condition of the Lagrange function for calculating the optimal solution of ${}^{\mathrm{H}}\mathrm{P}_{\mathrm{HC}}$ is that

$$\frac{\partial L}{\partial\,{}^{H}P_{HC}} = \left[{}^{H}F_S\times\right]^T\left(\left[{}^{H}F_S\times\right]{}^{H}P_{HC} + {}^{H}M_f\right) + \lambda\,S\,{}^{H}P_{HC} = 0 \quad (8)$$

$$\frac{\partial L}{\partial\lambda} = \frac{1}{2}\left(\left\|S\,{}^{H}P_{HC}\right\|^2 - r^2\right) \quad (9)$$

Furthermore, the second order partial derivative of the Lagrange function about the ${}^{\mathrm{H}}\mathrm{P}_{\mathrm{HC}}$ can be formulated as

$$\frac{\partial^2 L}{\partial\,{}^{H}P_{HC}{}^2} = \left[{}^{H}F_S\times\right]^T\left[{}^{H}F_S\times\right] + \lambda\,S \quad (10)$$

Thus,

$$x^T\frac{\partial^2 L}{\partial\,{}^{H}P_{HC}{}^2}x = \left\|{}^{H}F_S\times x\right\|^2 + \lambda\|Sx\|^2 \quad (11)$$

The second necessary condition of the Lagrange function can be described as

$$x^T\frac{\partial^2 L}{\partial\,{}^{H}P_{HC}{}^2}x > 0 \quad x\neq 0\in X$$

$$X \coloneqq \left\{x\middle|\left(S\,{}^{H}P_{HC}\right)^T x = 0\right\} \quad (12)$$

It is possible to derive the analytical solution of the problem to satisfy these two conditions.

By multiplying the ${}^{\mathrm{H}}\mathrm{F}_{\mathrm{S}}{}^{\mathrm{T}}$ on the left side of the Eq. (8), we get

$${}^{H}F_S{}^T\left\{-{}^{H}F_S\times\left({}^{H}F_S\times{}^{H}P_{HC} + {}^{H}M_f\right) + \lambda S\,{}^{H}P_{HC}\right\} = \lambda\,{}^{H}F_S{}^T S\,{}^{H}P_{HC} = 0 \quad (13)$$

Therefore, it is obvious that the optimal solution can be solved in terms of two situations $\lambda = 0$ and ${}^{\mathrm{H}}\mathrm{F}_{\mathrm{S}}{}^{\mathrm{T}}\mathrm{S}\,{}^{\mathrm{H}}\mathrm{P}_{\mathrm{HC}} = 0$.

***case* 1**: $\lambda = 0$

Eq. (8) becomes

$$-{}^{H}F_S\times\left({}^{H}F_S\times{}^{H}P_{HC} + {}^{H}M_f\right) = 0 \quad (14)$$

Based on Eq. (14), ${}^{\mathrm{H}}\mathrm{P}_{\mathrm{HC}}$ can be formulated as

$${}^{\mathrm{H}}\mathrm{P}_{\mathrm{HC}} = \frac{1}{\left\|{}^{\mathrm{H}}\mathrm{F}_{\mathrm{S}}\right\|^2}\left\{{}^{\mathrm{H}}\mathrm{F}_{\mathrm{S}}\times{}^{\mathrm{H}}\mathrm{M}_{\mathrm{f}} + \left({}^{\mathrm{H}}\mathrm{F}_{\mathrm{S}}{}^{\mathrm{T}}\,{}^{\mathrm{H}}\mathrm{P}_{\mathrm{HC}}\right){}^{\mathrm{H}}\mathrm{F}_{\mathrm{S}}\right\} \quad (15)$$

By substituting Eq. (15) into $\mathrm{g}\left(\mathrm{S}\,{}^{\mathrm{H}}\mathrm{P}_{\mathrm{HC}}\right)$ of the Constraint I and solving the new $\mathrm{g}\left(\mathrm{S}\,{}^{\mathrm{H}}\mathrm{P}_{\mathrm{HC}}\right)$ with variable ${}^{\mathrm{H}}\mathrm{F}_{\mathrm{S}}{}^{\mathrm{T}}\,{}^{\mathrm{H}}\mathrm{P}_{\mathrm{HC}}$, we can get the ${}^{\mathrm{H}}\mathrm{F}_{\mathrm{S}}{}^{\mathrm{T}}\,{}^{\mathrm{H}}\mathrm{P}_{\mathrm{HC}}$. Therefore, Eq. (15) becomes Eq. (16).

$${}^{\mathrm{H}}\mathrm{P}_{\mathrm{HC}} = \frac{{}^{\mathrm{H}}\mathrm{F}_{\mathrm{S}}\times{}^{\mathrm{H}}\mathrm{M}_{\mathrm{f}}}{\left\|{}^{\mathrm{H}}\mathrm{F}_{\mathrm{S}}\right\|^2} + \frac{{}^{\mathrm{H}}\mathrm{F}_{\mathrm{S}}}{\left\|{}^{\mathrm{H}}\mathrm{F}_{\mathrm{S}}\right\|^2}\left\{\frac{-{}^{\mathrm{H}}\mathrm{F}_{\mathrm{S}}{}^{\mathrm{T}}\mathrm{S}\left({}^{\mathrm{H}}\mathrm{F}_{\mathrm{S}}\times{}^{\mathrm{H}}\mathrm{M}_{\mathrm{f}}\right)\pm\sqrt{\mathrm{W}}}{\left\|\mathrm{S}\,{}^{\mathrm{H}}\mathrm{F}_{\mathrm{S}}\right\|^2}\right\} \quad (16)$$

where

$$\mathrm{W} = \left\|{}^{\mathrm{H}}\mathrm{F}_{\mathrm{S}}{}^{\mathrm{T}}\mathrm{S}\left({}^{\mathrm{H}}\mathrm{F}_{\mathrm{S}}\times{}^{\mathrm{H}}\mathrm{M}_{\mathrm{f}}\right)\right\|^2 - \left\|\mathrm{S}\,{}^{\mathrm{H}}\mathrm{F}_{\mathrm{S}}\right\|^2\left(\left\|\mathrm{S}\left({}^{\mathrm{H}}\mathrm{F}_{\mathrm{S}}\times{}^{\mathrm{H}}\mathrm{M}_{\mathrm{f}}\right)\right\|^2 - \mathrm{r}^2\left\|{}^{\mathrm{H}}\mathrm{F}_{\mathrm{S}}\right\|^4\right)$$

By multiplying Eq. (16) with ${}^{\mathrm{H}}\mathrm{F}_{\mathrm{S}}{}^{\mathrm{T}}\mathrm{S}$ and imposing the Constraint II, we will get Eqs. (17) and (18).

$${}^{H}F_S{}^T S\,{}^{H}P_{HC} = \frac{-\sqrt{W}}{\left\|S\,{}^{H}F_S\right\|^2} \quad (17)$$

$${}^{H}P_{HC} = \frac{{}^{H}F_S\times{}^{H}M_f}{\left\|{}^{H}F_S\right\|^2} + \frac{{}^{H}F_S}{\left\|{}^{H}F_S\right\|^2}\left\{\frac{-{}^{H}F_S{}^T S\left({}^{H}F_S\times{}^{H}M_f\right)-\sqrt{W}}{\left\|S\,{}^{H}F_S\right\|^2}\right\} \quad (18)$$

Note that in Eq. (18), since that it is necessary to make interior of the square root be positive so that we can get the optimal solution, Eq. (19) needs to be satisfied.

$$\alpha = \frac{1}{\left\|S\,{}^{H}F_S\right\|^2}\sqrt{N} \qquad r\left\|{}^{H}F_S\right\|^2 > \alpha \quad (19)$$

Where $\mathrm{N} = \left\|\mathrm{S}\,{}^{\mathrm{H}}\mathrm{F}_{\mathrm{S}}\right\|^2\left\|\mathrm{S}\left({}^{\mathrm{H}}\mathrm{F}_{\mathrm{S}}\times{}^{\mathrm{H}}\mathrm{M}_{\mathrm{f}}\right)\right\|^2 - \left\|{}^{\mathrm{H}}\mathrm{F}_{\mathrm{S}}{}^{\mathrm{T}}\mathrm{S}\left({}^{\mathrm{H}}\mathrm{F}_{\mathrm{S}}\times{}^{\mathrm{H}}\mathrm{M}_{\mathrm{f}}\right)\right\|^2$

***case* 2**: ${}^{H}F_S{}^T S\,{}^{H}P_{HC} = 0$

Because ${}^{H}F_S{}^{T}\,{}^{S}P_{HC} = 0$, the Constraint II is satisfied. The inner product of Eq. (8) and ${}^{S}P_{HC}$ can be formulated as

$$\begin{aligned}&\left(S^{H}P_{HC}\right)^{T}\left\{-{}^{H}F_S\times\left({}^{H}F_S\times{}^{H}P_{HC}+{}^{H}M_f\right)\right.\\&\left.+\lambda S^{H}P_{HC}\right\}\\&=\left(\left\|{}^{H}F_S\right\|^2+\lambda\right)r^2-\left(S^{H}P_{HC}\right)^{T}\left({}^{H}F_S\times{}^{H}M_f\right)=0\end{aligned}\tag{20}$$

Considering the fact that ${}^{H}P_{HC} = {}^{S}P_{HC} + l_Z$, the cross product of Eq. (8) and ${}^{S}P_{HC}$ is

$$\begin{aligned}&\left(S^{H}P_{HC}\right)\times\left\{-{}^{H}F_S\times\left({}^{H}F_S\times{}^{H}P_{HC}+{}^{H}M_f\right)\right.\\&\left.+\lambda S^{H}P_{HC}\right\}\\&=\left(S^{H}P_{HC}\right)\times\left\{-\left({}^{H}F_S{}^{T}l_Z\right){}^{H}F_S+\left\|{}^{H}F_S\right\|^2l_Z-\right.\\&\left.\left({}^{H}F_S\times{}^{H}M_f\right)\right\}=0\end{aligned}\tag{21}$$

The inner product of l_Z and Eq. (8) can be formulated as

$$\begin{aligned}&-\left({}^{H}F_S{}^{T}l_Z\right)l_Z^{T}\,{}^{H}F_S+\left\|{}^{H}F_S\right\|^2l_Z^{T}l_Z-l_Z^{T}\left({}^{H}F_S\times{}^{H}M_f\right)\\&=0\end{aligned}\tag{22}$$

by considering ${}^{H}P_{HC} = {}^{S}P_{HC} + l_Z$.

Set the $l_Z = p_Z e_z$, where $e_z = [0\ 0\ 1]^T$. Based on Eq. (22), the solution of p_Z can be concluded as

$$P_Z = 0,\quad P_Z = \frac{e_z{}^{T}\left({}^{H}F_S\times{}^{H}M_f\right)}{\left\|{}^{S}P_{HC}\right\|^2}\tag{23}$$

Let $C = -\left({}^{H}F_S{}^{T}l_Z\right){}^{H}F_S+\left\|{}^{H}F_S\right\|^2l_Z-\left({}^{H}F_S\times{}^{H}M_f\right)$. From Eq. (21), C is parallel to the ${}^{S}P_{HC}$. Based on the Constraint I

$$S^{H}P_{HC} = \pm r\frac{C}{\|C\|}\tag{24}$$

In term of calculating the inner product of the ${}^{S}P_{HC}$ and C, we get

$$\left(S^{H}P_{HC}\right)^{T}C = -\left(S^{H}P_{HC}\right)^{T}\left({}^{H}F_S\times{}^{H}M_f\right)\tag{25}$$

Based on Eqs. (20) and (25), it is concluded that

$$\lambda = -\left\|{}^{H}F_S\right\|^2\mp\frac{\|C\|}{r}\tag{26}$$

On the other hand, by substituting the $l_Z = p_Z e_z$ into the C and reorganizing the formula, it is found that $\|C\| = \alpha$. Note that, the equation of C after substituting the l_Z states that the result of which $P_Z = \frac{e_z{}^{T}\left({}^{H}F_S\times{}^{H}M_f\right)}{\left\|{}^{S}P_{HC}\right\|^2}$ actually contains the result of which $P_Z = 0$.

In order to satisfy the second order necessary condition defined in Eqs. (11) and (12), λ becomes $\lambda = -\left\|{}^{H}F_S\right\|^2+\frac{\|C\|}{r}$ and $r\left\|{}^{H}F_S\right\|^2<\alpha$ need to be satisfied. ${}^{H}P_{HC}$ can be formulated as

$${}^{H}P_{HC} = S^{H}P_{HC} + l_Z = -r\frac{C}{\|C\|}+l_Z\tag{27}$$

In conclusion, when $r\left\|{}^{H}F_S\right\|^2>\alpha$, ${}^{H}P_{HC}$ needs to satisfy Eq. (18). When $r\left\|{}^{H}F_S\right\|^2<\alpha$, ${}^{H}P_{HC}$ needs to satisfy Eq. (27).

3.3 Estimation of the Contact Position and Force When Contact with Two Point

As the analysis shown in Ref. [7], some D.O.Fs of the human body can be reduced when computing the control input. Thus, in order to analyze easily, we regard the human body as a simple pipe as in Fig. 4.

Based on the estimation of one point contact, it is possible to estimate the contact position and force

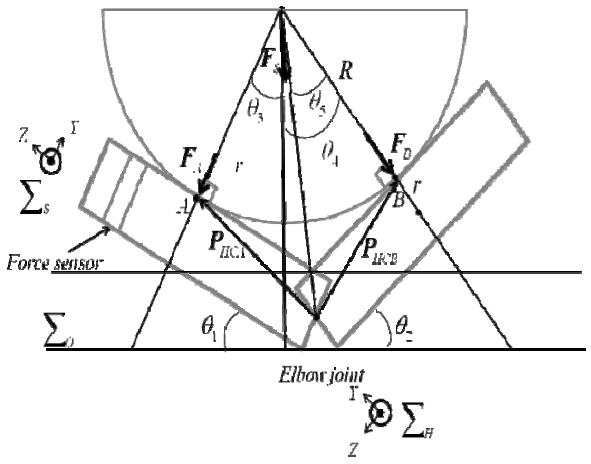

Fig. 4 Two contact point model.

when the robot arm contacts the object with two points. When there are two contact positions, according to Fig. 4, we have

$$F_S = F_A + F_B,$$
$$M_f = P_A \times F_A + P_B \times F_B \quad (28)$$

where F_S and M_f represent the force and moment measured by sensor. P_A and P_B are the vectors from sensor's center to points A and B. F_A and F_B are forces acting on the points.

From Fig. 4, it is known that

$$\|F_A\| = \|F_S\| \cos\theta_3, \ \|F_B\| = \|F_S\| \cos\theta_4 \quad (29)$$

where $\theta_3 = \theta_1$, $\theta_4 = \theta_2$ and $\theta_5 = \frac{1}{2}(\theta_3 + \theta_4)$.

Let the ${}^{H}P_{HCA}$ and ${}^{H}P_{HCB}$ denote the vector from the origin of the flexion axis coordinate system and the points A and B.

$${}^{H}P_{HCA} = \begin{pmatrix} r \\ R\tan\theta_5 + r\tan\theta_5 \end{pmatrix}$$

$${}^{H}P_{HCB} = \begin{pmatrix} r \\ -(R\tan\theta_5 + r\tan\theta_5) \end{pmatrix}$$

$${}^{H}P_{HCB} = {}^{H}R_S\,{}^{S}P_{HCA} \quad (30)$$

It is known that $\|{}^{H}P_{HCA}\| = \|{}^{H}P_{HCB}\|$.

3.4 Estimation of Physical Parameter Using Dual-arm

Since it is necessary to complete a work in cooperation using dual arm for a nursing care robot, the estimation of physical parameter using dual arm is very important.

3.4.1 Coordinate Transformation of the Contact Position and Force

The contact force F_S and contact position P_{HC} in the sensor coordinate system can be represented as

$${}^{S}P_{SC} = {}^{S}R_E\left({}^{E}R_H P_{HC} + {}^{E}P_{EH}\right) + {}^{S}P_{SE}$$
$${}^{S}F_S = {}^{S}R_E\,{}^{E}R_H F_S \quad (31)$$

3.4.2 Estimation of the Cylinder's Center of Gravity

F_R and F_L denote respectively the forces action at the right and left arm. L_L, L_R denote the distance from contract position to the center of gravity. Thus, we can get

$$L_{RL} = L_L + L_R, \quad \|F_R\|L_R = \|F_L\|L_L \quad (32)$$

Hence, it is concluded that

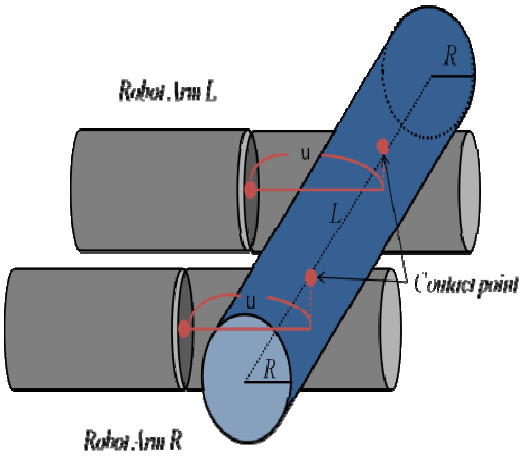

Fig. 5 Single contact point.

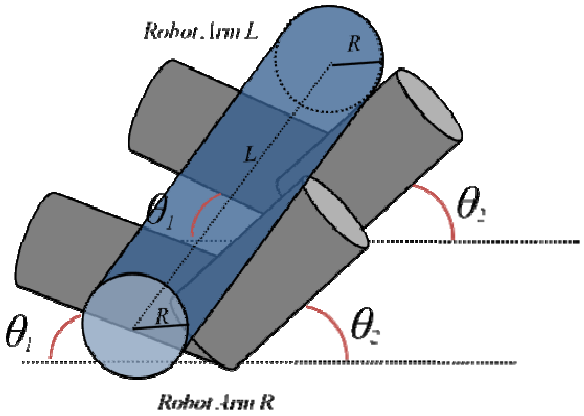

Fig. 6 Dual contact point.

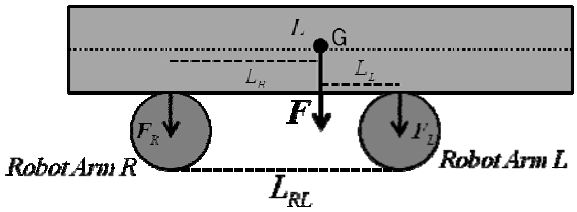

Fig. 7 Model of robot arms and circular cylinder.

$$L_R = \frac{\|F_L\|}{\|F_R\| + \|F_L\|}L_{RL} = \frac{F_L}{\|F\|}L_{RL}$$
$$L_L = \frac{\|F_R\|}{\|F_R\| + \|F_L\|}L_{RL} = \frac{F_R}{\|F\|}L_{RL} \quad (33)$$

Since the center of gravity P_G can be represented as

$$P_G = {}^{o}P_{HC} + {}^{o}P_{CG}$$

where ${}^{o}P_{HC}$ represents the vector from the origin of the origin coordinate system to the contact position, ${}^{o}P_{CG}$ denotes the vector from contact position to center of gravity.

4. Simulation Result

4.1 The Setting of the Robot's Model

The model of the robot is used as a nursing care robot under development as shown in Fig. 1. The radius of the robot arm which regarded as a cylinder shape is setting as 0.05 m. The relation parameter between each coordinate system is shown in Table 1. The gravity acceleration is $g = 9.8\, m/s^2$. Moreover, since there are noises in the force and moment measured by the 6-axis force sensor, it is necessary to add random noises with a normal distribution.

4.2 The Model Settings of the Object

The coordinate system as shown in Fig. 8 is used. The rotation matrix between the coordinate systems is shown in Table 2 and the mechanical part that 10° of the shoulder and 30° of the arm have not been shown in the table. The physical parameters which the length $L = 1\, m$, radius is $R = 0.0825\, m$, mass is $M = 3.8\, kg$ have already been known. The distance between two contact point is $L_{RL} = 0.597\, m$. The posture of the robot has already set as two situations: contact object with (1) single point (2) dual points.

4.2.1 Single Point

The posture of robot is shown in Fig. 5 and is fixed. The distance between origin of flexion axis coordinate system and object is denoted as u. This simulation is performed with altering u in two situations: (a) u = 0.10 m (b) u = 0.25 m.

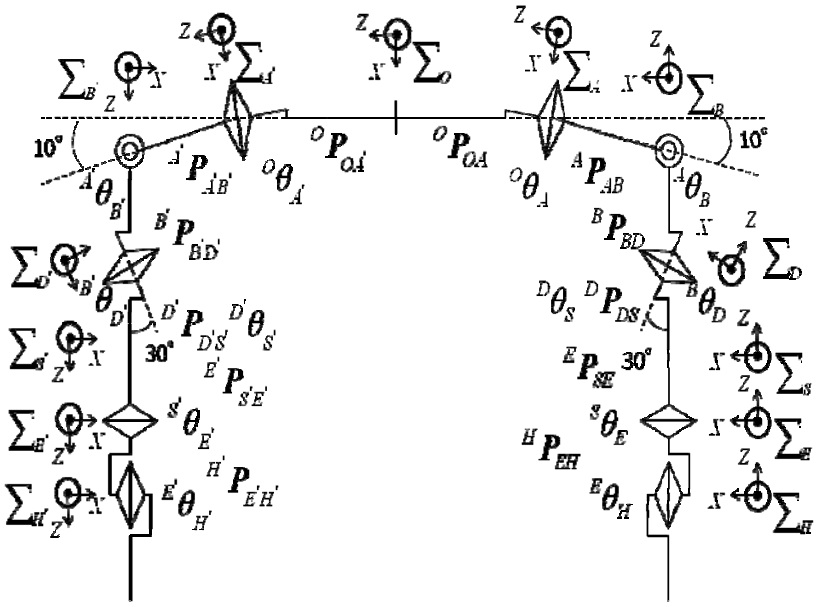

Fig. 8 Model of robot with arms.

Table 1 Link vector of robot links.

Right arm	[m]	Left arm	[m]
${}^{O}\mathbf{P}_{OA'}$	$[0 \quad 0 \quad -0.2]^T$	${}^{O}\mathbf{P}_{OA}$	$[0 \quad 0 \quad 0.2]^T$
${}^{A'}\mathbf{P}_{A'B'}$	$[0 \quad 0 \quad -0.1]^T$	${}^{A}\mathbf{P}_{AB}$	$[0 \quad 0 \quad 0.1]^T$
${}^{B'}\mathbf{P}_{B'D'}$	$[0 \quad 0 \quad -0.1]^T$	${}^{B}\mathbf{P}_{BD}$	$[0 \quad 0 \quad -0.1]^T$
${}^{D'}\mathbf{P}_{D'S'}$	$[0 \quad 0 \quad -0.11]^T$	${}^{D}\mathbf{P}_{DS}$	$[0 \quad 0 \quad 0.11]^T$
${}^{S'}\mathbf{P}_{S'E'}$	$[0 \quad 0 \quad -0.045]^T$	${}^{S}\mathbf{P}_{SE}$	$[0 \quad 0 \quad 0.045]^T$
${}^{E'}\mathbf{P}_{E'H'}$	$[0 \quad 0 \quad -0.07]^T$	${}^{E}\mathbf{P}_{EH}$	$[0 \quad 0 \quad 0.07]^T$

Table 2 Rotation matrix of robot links.

	${}^{O}\theta_{A}$ ${}^{O}\theta_{A'}$	${}^{A}\theta_{B}$ ${}^{A'}\theta_{B'}$	${}^{B}\theta_{D}$ ${}^{B'}\theta_{D'}$	${}^{D}\theta_{S}$ ${}^{D'}\theta_{S'}$	${}^{S}\theta_{E}$ ${}^{S'}\theta_{E'}$	${}^{E}\theta_{H}$ ${}^{E'}\theta_{H'}$
(1)	90	-80	0	0	0	0
	90	80	0	0	0	0
(2)	60	-80	0	0	0	90
	60	80	0	0	0	-90

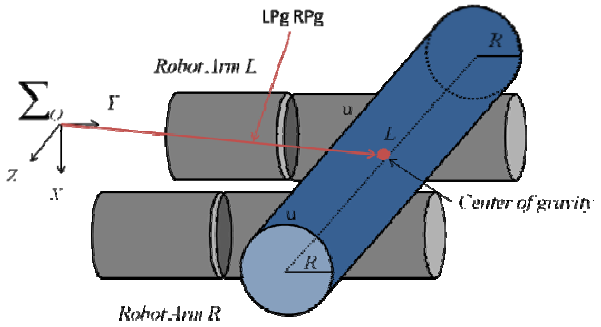

Fig. 9 Relationship LPg and RPg and model.

4.2.2 Dual Points

As shown in Fig. 6, each arm contacts the object with two points by bending the arm in order to sandwich the object. Note that, θ_1, θ_2 in Fig. 6 are 30° and 60° respectively.

4.3 Results of Simulation

In the situation of 4.2.1, each component of the position vector from the origin of the origin coordinate system to the object's gravity center has been estimated basing on the information measured by left and right sensor.

Besides, in the situation of 4.2.2, each component of the position vectors from origin of the origin coordinate system to the object's gravity center, denoted as LAP g, LBP g, RAP g and RBP g, are also estimated and shown below.

4.3.1 Simulation Result of Single Contact Point

Figs. 10 and 11 show the results of a) with u = 0.1 m.

From Figs. 10 and 11, none of the components of the position vectors which are estimated by the force sensor has a large fluctuation due to the existence of the noises. The two situations both have the maximum error 0.2 mm on z-component.

Figs. 12 and 13 show the results of a) with u = 0.25 m. There is also none large fluctuation in the results and

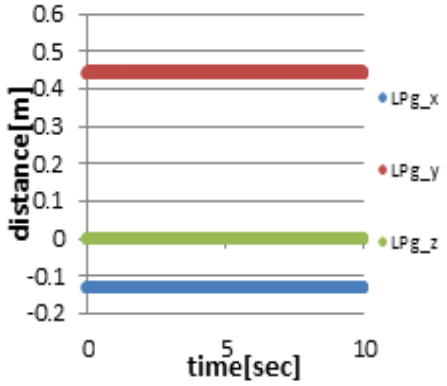

Fig. 10 Estimated vector from the origin to center of gravity (by left).

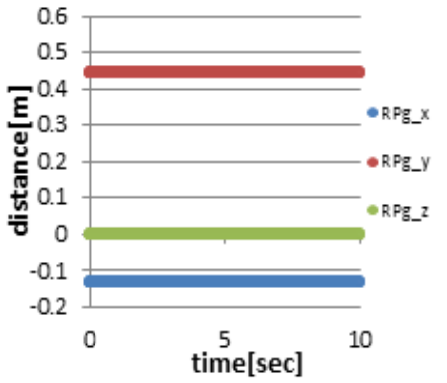

Fig. 11 Estimated vector from the origin to center of gravity (by right).

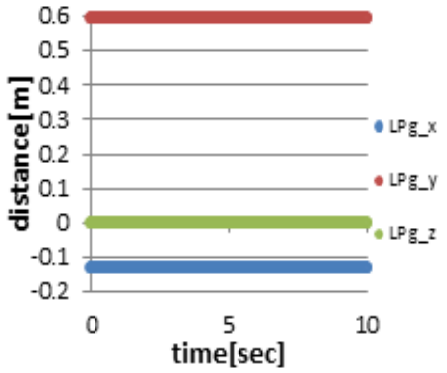

Fig. 12 Estimated vector from the origin to center of gravity (by left).

the maximum error at this situation is also 0.2 mm on z-component.

4.3.2 Simulation Result of Dual Contact Point

From Figs. 14-17, the components of each vector measured by left and right force sensors contain no large fluctuation. The errors of the estimated vectors mainly come from the z-component. The maximum error is about 0.3 mm.

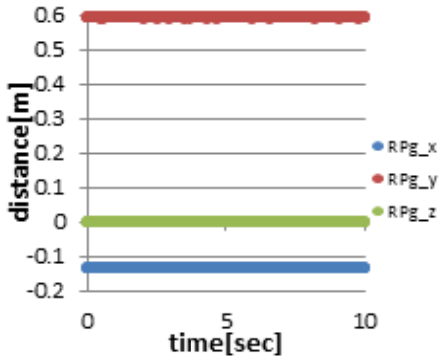

Fig. 13 Estimated vector from the origin to center of gravity (by right).

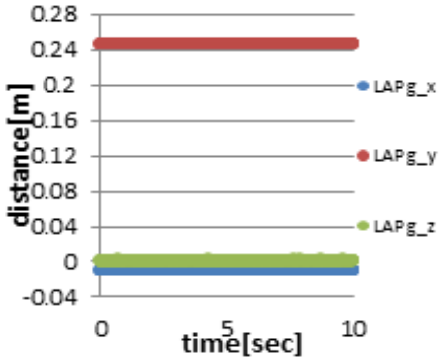

Fig. 14 Estimated vector from the origin to center of gravity (by left point A).

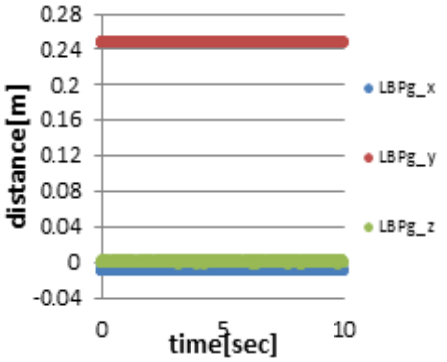

Fig. 15 Estimated vector from the origin to center of gravity (by left point B).

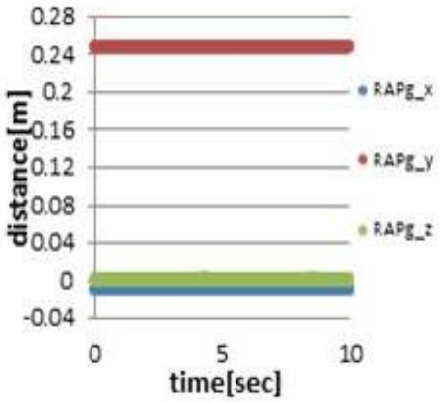

Fig. 16 Estimated vector from the origin to center of gravity (by right point A).

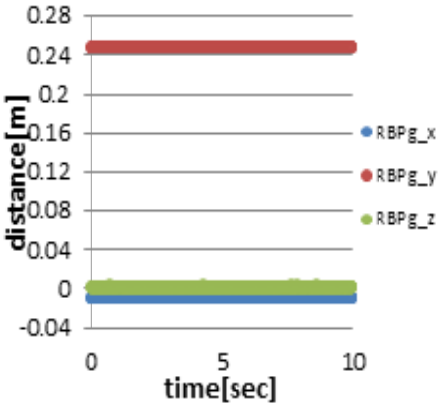

Fig. 17 Estimated vector from the origin to center of gravity (by right point B).

5. Experiment

5.1 The Setting of the Experiment

We use the cylindrical object in the experiment as Fig. 18. It has the parameters of radius $R = 0.0825\ m$, length $L = 1\ m$, mass $M = 3.8\ kg$.

5.2 Results of the Experiment

5.2.1 Single Contact Point

Figs. 19-22 show the results of the experiment of single contact point with the setting u = 0.10 m and u = 0.25 m. From these figures, it is known that there is no large fluctuation in the results. The error results show that there is strong correlation between the error and the value of distance u. Error becomes larger with the increase of the value u.

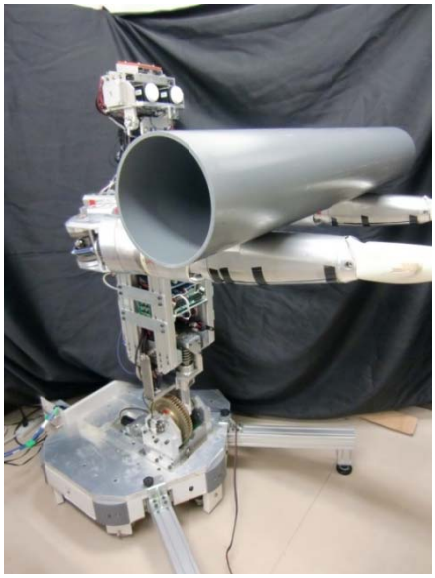

(a)

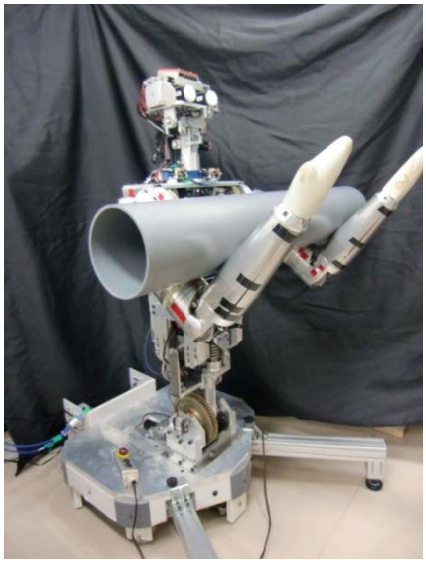

(b)

Fig. 18 Experiment scene.

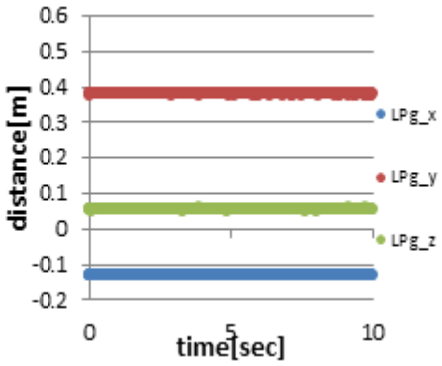

Fig. 19 Estimated vector from the origin to center of gravity (by left).

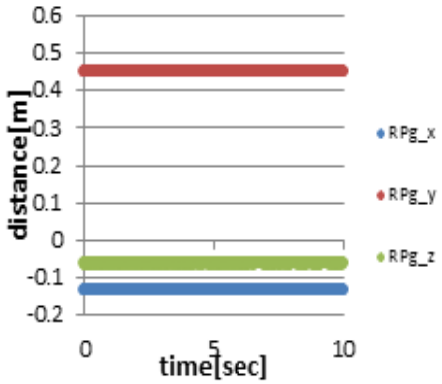

Fig. 20 Estimated vector from the origin to center of gravity (by right).

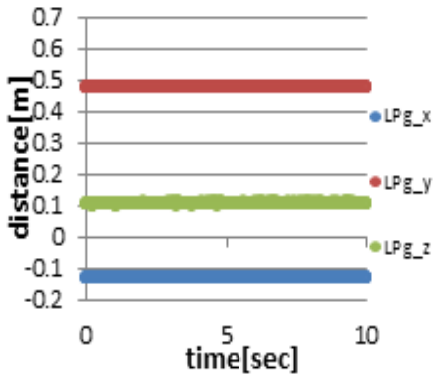

Fig. 21 Estimated vector from the origin to center of gravity (by left).

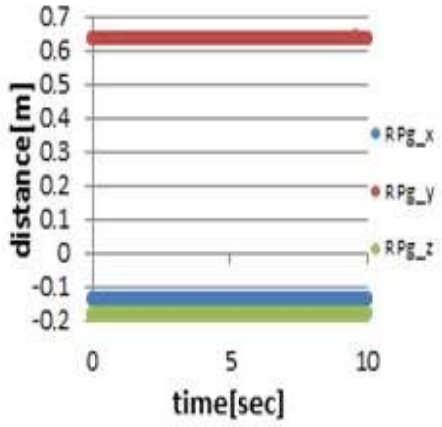

Fig. 22 Estimated vector from the origin to center of gravity (by right).

Moreover, since the robot arm is not a perfect cylinder, it appears more errors in *y* and *z* component than simulation's result when performing the experiment. We can believe that the model error has a big effect on the result of the estimation.

5.2.2 Dual Contact Points

Figs. 23-26 show the results of the experiment of dual contact point with the setting u = 0.10 m and u = 0.25 m. The results show that there is also no large fluctuation in each component. It is known that there is no error in the x and y components and there are errors of about 3.2 cm estimated by left force sensor and 5.7 cm estimated by right force sensor in z-component.

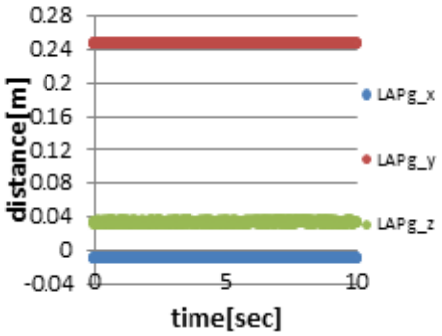

Fig. 23 Estimated vector from the origin to center of gravity (by left point A).

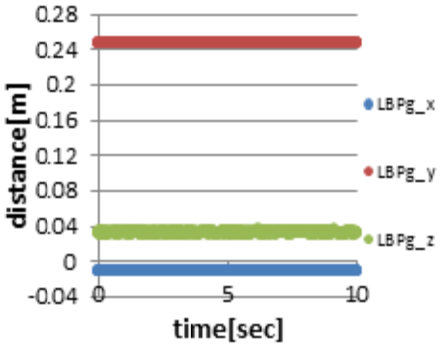

Fig. 24 Estimated vector from the origin to center of gravity (by left point B).

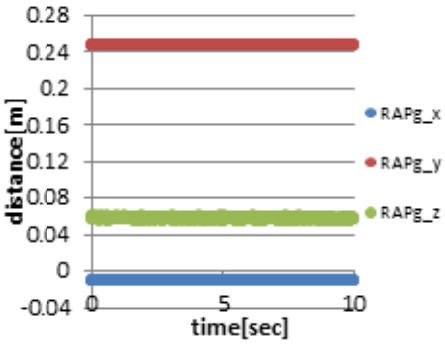

Fig. 25 Estimated vector from the origin to center of gravity (by right point A).

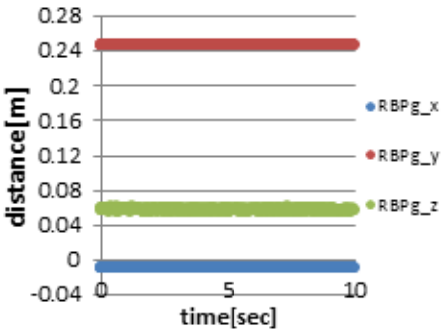

Fig. 26 Estimated vector from the origin to center of gravity (by right point B).

6. Conclusions

In this research, the estimation of the position of object's center of gravity has been performed using the sensors installed on the nursing care robot under development. In order to verify the effectiveness of the research, we perform the simulation and experiment for two situations (single contact point and dual contact point).

The results of simulation and experiment show that it can steady estimate the position of gravity center with little error. From the experiment, the results also show the correlation between the u, which denote the distance between origin of flexion axis coordinate system and object, and the error. If u increases, the error becomes larger. Besides, the model errors of the robot also bring some effects on the estimation. Hence, in the future work, it is necessary to correct the model of the robot so as to estimate more accurate.

References

[1] Asano, F., LUO, Z. W., Yamakita, M., and Hosoe, S. 2005. "Modeling and Bio-mimetic Control for Whole-Arm Dynamic Cooperative Manipulation." *Advanced Robotics* 19 (9): 929-50.

[2] Odashima, T., Onishi, M., and Tahara, K. 2006. "A Soft Human-Interactive Robot Ri-man." Intelligent Robots and Systems, 2006 IEEE/RSJ International Conference on. IEEE.

[3] Onishi, M., LUO, Z. W., Odashima, T., Hilrano, S., Tahara, K., and Mukai, T. 2007. "Generation of Human Care Behaviors by Human-Interactive Robot RI-man." Robotics and Automation, 2007 IEEE International Conference on. IEEE.

[4] Asano, F., Luo, Z. W., Yamakita. M. et al. 2005. "Modeling and Bio-mimetic Control for Whole-Arm Dynamic Cooperative Manipulation." *Advanced Robotics* 19 (9): 929-50.

[5] Mukai, T., and Kato, Y. 2008. "1 ms Soft Areal Tactile Giving Robots Soft Response." *Journal of Robotics and Mechatronics* 20 (3): 473-80.

[6] Nagase, K., Yoshinaga, K., Nakashima, A., and Hayakawa, Y. 2005. "Estimation of Contact Point by Force Sensor with Measurement Noise." *Journal of the Robotics Society of Japan* 23 (6): 85-91.

[7] DONG, H. W., LUO, Z. W., and Nagano, A. 2010. "Reduced Model Adaptive Force Control for Carrying Human Beings with Uncertain Body Dynamics in Nursing Care." Advanced Intelligent Mechatronics (AIM), 2010 IEEE/ASME International Conference on. IEEE, 193-200.